

**This manuscript entitled “A machine learning approach for ozone forecasting and its application for Kennewick, WA” is a preprint** and will be submitted for publication in **Environmental Science and Technology** and then undergo the peer-review process. If accepted, the final version of this manuscript will be available via the ‘Peer-reviewed Publication DOI’ link on the right-hand side of this webpage. Please feel free to contact any of the authors and we welcome feedback. The authors and affiliations of the manuscript are:

Kai Fan

Laboratory for Atmospheric Research, Civil and Environmental Engineering, Washington State University

kai.fan@wsu.edu

Brian Lamb

Laboratory for Atmospheric Research, Civil and Environmental Engineering, Washington State University

blamb@wsu.edu

Ranil Dhammapala

Washington State Department of Ecology

ranil.dhammapala@ecy.wa.gov

Ryan Lamastro

State University of New York at New Paltz

lamastrr1@hawkmail.newpaltz.edu

Yunha Lee

Laboratory for Atmospheric Research, Civil and Environmental Engineering, Washington State University

yunha.lee@wsu.edu

1 A machine learning approach for ozone forecasting  
2 and its application for Kennewick, WA

3 *Kai Fan<sup>1</sup>, Ranil Dhammapala<sup>2</sup>, Ryan Lamastro<sup>3</sup>, Brian Lamb<sup>1</sup>, and Yunha Lee<sup>1\*</sup>*

4 *<sup>1</sup>Laboratory for Atmospheric Research, Civil and Environmental Engineering, Washington State*  
5 *University*

6 *<sup>2</sup>Washington State Department of Ecology*

7 *<sup>3</sup>State University of New York at New Paltz*

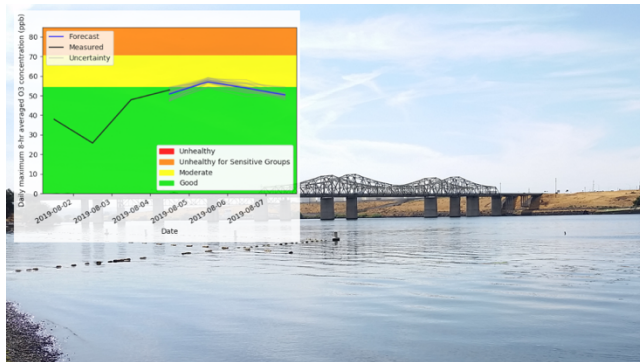
8 \*Corresponding Author

9 E-mail: [yunha.lee@wsu.edu](mailto:yunha.lee@wsu.edu) (Yunha Lee)

10  
11 **ABSTRACT:**

12 Chemical transport models (CTM) are widely used for air quality modeling, but these models miss  
13 forecasting some air pollution events, and require a lot of computational power. In Kennewick,  
14 WA, elevated O<sub>3</sub> episodes can occur during the summer and early fall, but the CTM-based  
15 operational forecasting system (AIRPACT) struggles to capture them. This research used the 2015  
16 – 2018 historical archives from the Weather Research and Forecasting (WRF) meteorological  
17 model forecasts produced daily by the University of Washington, and O<sub>3</sub> observation data at

18 Kennewick to train two machine learning modeling frameworks, ML1 and ML2 for a reliable  
19 forecasting system. ML1 used the random forest (RF) classifier and multiple linear regression  
20 (MLR) models, and ML2 used a two-phase RF regression model with best-fit weighting factors.  
21 Since April 2019, the ML modeling frameworks have been used to produce daily 72-hour O<sub>3</sub>  
22 forecasts and have provided the forecasts via the web for the agency and public use. For the peak  
23 O<sub>3</sub> days, AIRPACT showed a large variation, while ML2 underpredicted and ML1 performed the  
24 best. In the future, this dual ML forecast system will be applied to other locations within the Pacific  
25 Northwest.



26

## 27 1. INTRODUCTION

28 Chemical transport models (CTM) are widely used to simulate the temporal and spatial variation  
29 of air quality.<sup>1</sup> CTMs include various atmospheric physical and chemical processes as well as  
30 sources and sinks. However, not every physical and chemical process in the atmosphere has been  
31 understood.<sup>2</sup> Even though the accuracy of numerical models keeps improving, there are still large  
32 uncertainties and errors in the simulations. For the CTMs, the high computational cost is an  
33 additional concern.

34 The Air Indicator Report for Public Awareness and Community Tracking (AIRPACT) was  
35 developed for air quality forecasting in the Pacific Northwest in the U.S. AIRPACT uses the  
36 Community Multiscale Air Quality Modeling System (CMAQ) model to compute air quality with  
37 the Weather Research and Forecasting (WRF) meteorology. The AIRPACT domain mainly covers  
38 Washington, Idaho and Oregon State with 4 km horizontal grid cells and 37 vertical levels. The  
39 hourly simulations use the Carbon Bond, version 5 (CB05) as the gas chemistry mechanism and  
40 AERO6 as the aerosol module. AIRPACT 48-hour forecasts are produced daily and provided via  
41 the web to the public and local air quality agencies (<http://lar.wsu.edu/airpact/>).

42 Within the AIRPACT domain, Kennewick is part of the Tri-cities metropolitan area with a total  
43 population of about 216,000 (Estimated population of Kennewick 83,670, Pasco 75,290 and  
44 Richland 56,850 in 2019).<sup>3</sup> The city is 32 km north of Washington State's southern border and is  
45 in a hot dry portion of the state. Recent monitoring and a large field study have shown that a few  
46 high O<sub>3</sub> events typically occur during summer and early fall.<sup>4</sup> While AIRPACT forecasts initially  
47 predicted the Tri-cities area as an ozone hotspot, the daily forecasts struggle to forecast correctly  
48 high O<sub>3</sub> concentrations in this area. There were 20 days when the air quality was unhealthy for  
49 sensitive groups in 2015 – 2018, but AIRPACT only captured one of them.

50 Machine learning (ML) models have been used to predict air quality in recent years. These  
51 methods incorporate a variety of features, including observed pollutant levels and various  
52 meteorological variables as the basis for training and applying ML methods. For example, Feng  
53 et al.<sup>5</sup> input trajectory-based geographic parameters, meteorological forecasts and associated  
54 pollutant predictors to an artificial neural network to predict PM<sub>2.5</sub> concentrations in Beijing,  
55 China. Freeman et al.<sup>6</sup> used a recurrent neural network with short-term memory to predict 72-hour  
56 O<sub>3</sub> forecasting with training via hourly air quality and meteorological data. Zamani Joharestani et

57 al.<sup>7</sup> tested three machine learning approaches, random forest, extreme gradient boosting and deep  
58 learning to predict the PM<sub>2.5</sub> concentrations in Tehran, Iran using 23 features.

59 A successful ML model must be trained with a large dataset. For air quality prediction, the  
60 training dataset usually includes meteorological data (temperature, relative humidity, pressure,  
61 wind speed and direction, etc.) and observed pollutant concentrations. However, compared to  
62 numerical models, ML methods tend to be more computationally efficient, require less input data,  
63 and perform better for specific events, which makes ML models popular in recent years.<sup>5,6,8-10</sup>

64 In this study, we developed ML modeling frameworks to predict O<sub>3</sub> mixing ratios, which were  
65 based on the following approaches: random forest (RF) and multiple linear regression (MLR). RF  
66 is one of the most popular machine learning methods and has been used in many air quality  
67 modeling and forecast studies. The RF method has been demonstrated to provide reliable forecasts  
68 for O<sub>3</sub> and PM<sub>2.5</sub> with lower computational cost compared to physical models.<sup>11-14</sup> RF consists of  
69 an ensemble of decision trees, and decision tree learning is for approximating discrete-valued  
70 functions.<sup>15-17</sup> The RF model can be used for classification and regression. For our study, the RF  
71 classifier model was used to predict the O<sub>3</sub> Air Quality Index (AQI) categories, and the RF  
72 regression model was used to predict O<sub>3</sub> mixing ratios. MLR is a regression method with one  
73 dependent variable and several independent variables, which we used to predict O<sub>3</sub> levels.  
74 Previous studies that used MLR models to predict O<sub>3</sub> mixing ratios showed performance as good  
75 as more complex machine learning models.<sup>18-21</sup> Yuchi et al.<sup>22</sup> used RF and MLR for indoor air  
76 quality forecasts, and RF showed better in-sample predictions, MLR showed better out-of-sample  
77 predictions. So, this paper will discuss the application of both RF and MLR for O<sub>3</sub> forecasts.

78 The goal of this study was to provide reliable air quality forecasts using machine learning  
79 approaches, especially for high O<sub>3</sub> events in Kennewick, WA. Section 2 presents the two machine

80 learning modeling frameworks we developed, including the training dataset. Section 3 presents the  
81 feature selection, evaluation of the model performance using 10-time 10-fold/walk-forward cross-  
82 validation and a summary of the forecast results in 2019.

83

## 84 **2. DATASETS AND MODELING FRAMEWORKS**

### 85 **2.1. Training dataset.**

86 The training dataset for our machine learning models includes the previous day's observed O<sub>3</sub>  
87 mixing ratios, time information (hour, weekday, month), and simulated meteorology from daily  
88 WRF forecasts from May to September in 2015 – 2018 at Kennewick, WA. Because the heat and  
89 sunlight favor the O<sub>3</sub> generation,<sup>23</sup> and wildfires can generate the O<sub>3</sub> precursors,<sup>24</sup> observations are  
90 only made from May to September. The training dataset covered this period. The WRF  
91 meteorology was obtained from the University of Washington,<sup>25,26</sup> which is used in AIRPACT as  
92 an input to generate emissions and air quality forecasting. We used the temperature, surface  
93 pressure, relative humidity, wind speed, wind direction, and planetary boundary layer height (PBL)  
94 in the training dataset. Time information was included in the training dataset due to the significant  
95 trend of O<sub>3</sub> variation in the diurnal, weekday and monthly scales. Table S1 summarizes the  
96 historical O<sub>3</sub> AQI during the training period. Here we define a high O<sub>3</sub> day as the day when the  
97 observed AQI category is worse than Moderate (i.e. AQI category 3 or worse). The high O<sub>3</sub> days  
98 in all the years used here are less than 5% of total simulated days, except for 2017. Extensive  
99 wildfires occurred in 2017, and there were 8 days that the air quality was unhealthy for sensitive  
100 groups (i.e., O<sub>3</sub> AQI category = 3). The days when the wildfire smoke caused excess O<sub>3</sub> were  
101 marked in the historical data, but it could not be involved in the training dataset because it was not

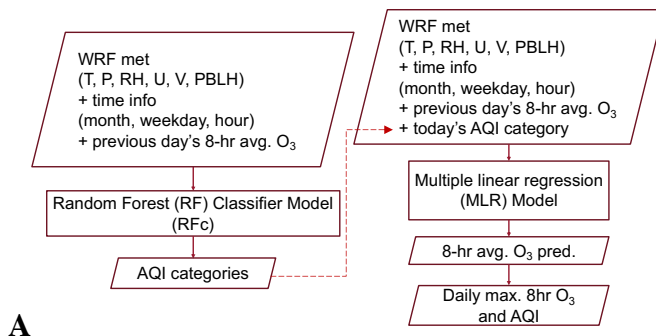
102 predictable. And there were only four days in this case, so it would not affect the model training  
103 significantly.

104

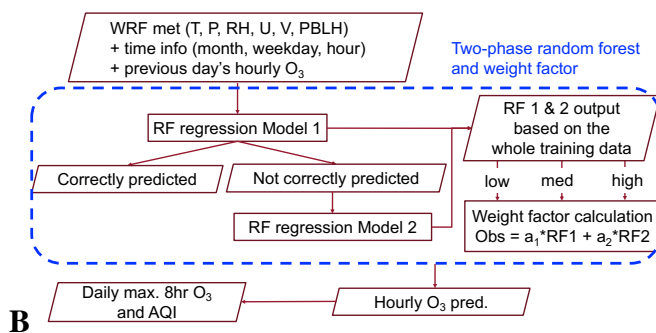
## 105 **2.2. Machine learning modeling frameworks**

106 We have developed two O<sub>3</sub> forecast modeling frameworks based on ML methods. The first  
107 machine learning modeling framework (ML1, hereafter; see Figure 1A) used RF classifier and  
108 MLR models. The *RandomForestClassifier* and *RFE* functions in the python module *sklearn* were  
109 used. In ML1, the WRF meteorology, time information, and previous day's 8-hour averaged O<sub>3</sub>  
110 mixing ratios were first used to train an RF classifier model to predict AQI categories. There are  
111 not many high O<sub>3</sub> cases, which makes the dataset imbalanced, and the imbalanced training data  
112 may lead the bias toward the low O<sub>3</sub> prediction.<sup>27</sup> To address the problem from the imbalanced  
113 data, the *balanced\_subsample* option was turned on for the RF classifier. The *balanced\_subsample*  
114 gives weights to the AQI category values based on their frequency in the bootstrap sample for each  
115 tree, so the high AQI values with low frequency in the training dataset are weighted proportionally  
116 more. Separately, the observed AQI categories were added to the training dataset to train the MLR  
117 model. When used for forecasting, the RF classifier model was first used to predict the AQI  
118 categories, which were in turn fed into the MLR model to predict the O<sub>3</sub> mixing ratios, as the red  
119 dashed line shown in Figure 1A.

120



121



122 **Figure 1.** (A) ML1 modeling framework based on random forest (RF) classifier and multiple linear  
 123 regression (MLR) models (B) ML2 based on a two-phase RF regression and weight factors

124

125 Machine Learning modeling framework 2 (ML2 hereafter; see Figure 1B) is based on a two-  
 126 phase random forest regression model. The *RandomForestRegressor* function in the python  
 127 module *sklearn* was used. ML2 used the WRF meteorology, time information, and previous day's  
 128 hourly O<sub>3</sub> mixing ratios to train an RF regression model to predict O<sub>3</sub> mixing ratios. The whole  
 129 historical dataset was used to train the first RF regression model (RF1 in Figure 1B). The training  
 130 data was isolated when RF1 predicted O<sub>3</sub> mixing ratios differed from the observations by more  
 131 than 5 ppb, and then the isolated dataset was used to train the second RF regression model (RF2  
 132 in Figure 1B). The training dataset for RF2 was a subset of the whole training data, so RF2 required  
 133 more decision trees (100 trees for RF1 and 200 trees for RF2).<sup>28</sup> This is why it is called a two-



134 phase RF regression model. The RF1 predicted O<sub>3</sub> mixing ratios were divided into three levels  
135 (low: < 30 ppb, medium: 30 – 50 ppb, high: > 50 ppb). For the data within each level, a set of  
136 weighting factors, a<sub>1</sub> and a<sub>2</sub>, were computed based on a linear regression equation,

$$137 \quad O_{3\text{observed}} = a_1 * RF_1 + a_2 * RF_2 \quad (1)$$

138 When doing forecasting, RF1 and RF2 were used to provide initial predictions. The RF1  
139 prediction determined which weighting factors would be used. The hourly O<sub>3</sub> prediction was  
140 computed as

$$141 \quad O_3 = a_1 * RF_1 + a_2 * RF_2 \quad (2)$$

142

### 143 **2.3. Ensemble forecasting system**

144 The ML1 and ML2 modeling frameworks have been used to provide 72-hour “ensemble”  
145 operational O<sub>3</sub> forecasts each day, by using more than 20 members from the  
146 University of Washington Mesoscale Ensemble system (<https://a.atmos.washington.edu/wrft/ensembles/info.html>) beginning in April 2019. We predicted the O<sub>3</sub> levels with each WRF member to  
147 compile a 72-hour ensemble mean forecast with an associated uncertainty range. The forecasts are  
148 available to the public on <http://ozonematters.com>, with the ability to sign up for email alerts if  
149 “Unhealthy for Sensitive Groups” or worse levels are forecast. To increase the size of the training  
150 dataset and improve the forecast accuracy, we included the new observational data from the  
151 previous day and re-trained the models daily. For the ensemble daily forecasts, the computational  
152 time is approximately 1 min for ML1 and less than 3 min for ML2.  
153

154

## 155 2.4. Statistical methods for O<sub>3</sub> AQI evaluation

156 Two parameters, Heidke Skill Score (HSS) and the Hanssen-Kuiper Skill Score (KSS) were used  
157 to evaluate the machine learning model prediction. Table S2 is a 2x2 contingency table, which  
158 shows the simple yes or no cases.<sup>29</sup> For the air quality research, “yes” usually means air pollution  
159 events, and “no” means good air quality. The equations (3) and (4) show how HSS and KSS are  
160 computed.<sup>30</sup>

$$161 \quad HSS = \frac{a + d - a_r - d_r}{n - a_r - d_r} \quad (3)$$

$$162 \quad \text{Where } a_r = \frac{(a+b)(a+c)}{n}, d_r = \frac{(b+d)(c+d)}{n}$$

$$163 \quad KSS = \frac{ad - bc}{(b + d)(a + c)} \quad (4)$$

164 HSS represents the accuracy of the model prediction compared with a reference forecast (r in  
165 equation 3), which is from the random guess that is statistically independent of the observations.<sup>30,31</sup>  
166 The range of the HSS is from  $-\infty$  to 1. A negative value means a random guess is better, 0 means  
167 no skill, and 1 means a perfect score. KSS measures the ability to separate different categories.  
168 The range is from -1 to 1 where 0 means no skill, and 1 means a perfect score.

169 For the multi-category case in this research with AQI 1 (Good), 2 (Moderate) or 3 (Unhealthy  
170 for Sensitive Groups), we use the 3x3 contingency table in Table S3<sup>32</sup>. The skill scores are  
171 computed as follows.<sup>30</sup>

$$172 \quad HSS = \left( \sum_{i=1}^3 p_{ii} - \sum_{i=1}^3 p_i \hat{p}_i \right) / \left( 1 - \sum_{i=1}^3 p_i \hat{p}_i \right) \quad (5)$$

$$173 \quad KSS = \left( \sum_{i=1}^3 p_{ii} - \sum_{i=1}^3 p_i \hat{p}_i \right) / \left( 1 - \sum_{i=1}^3 p_i p_i \right) \quad (6)$$

174 The  $p_{ii}$  is the sample frequency when the observed and model predicted AQI is  $i$ , and  $p_i$  and  $\hat{p}_i$   
175 are the observed and model predicted sample frequency when AQI =  $i$ . The multi-category case is  
176 based on the simple yes or no case, and the skill scores, HSS and KSS have the same meaning as  
177 the simple case.

178

## 179 **3. RESULTS AND DISCUSSION**

### 180 **3.1. Feature selection for machine learning models**

181 There were 10 features for the RF classifier and regression model and 11 features for the MLR  
182 model. Too many features can cause an overfitting problem,<sup>33</sup> so the attributes  
183 *feature\_importances\_* in function *RandomForestClassifier/RandomForestRegressor* and *ranking\_*  
184 in *RFE* were used to do the feature selection. The selected features were input to train the model.

185 There were two components in ML1, RF classifier and MLR model. For an RF model, the feature  
186 selection function with the default setting computed the importance weights, and the features  
187 whose weight was above the mean weight were selected. The feature weights could change in each  
188 training process, but the ranking showed very little variation. The previous day O<sub>3</sub> observation,  
189 temperature and hour were the primary features selected, and the relative humidity was selected in  
190 some cases. The default number of selected features for MLR was half of the total features  
191 available, so two more features were chosen by the built-in feature selection function, in addition  
192 to the three primary features: the previous day O<sub>3</sub> observation, temperature, relative humidity, AQI  
193 category, and surface pressure. The output of each framework was hourly O<sub>3</sub> mixing ratios for

194 each 72-hour forecast. For evaluation purposes, these forecast values were compiled into the  
195 maximum daily 8-hour moving average O<sub>3</sub> (MDA8).

196 The feature selection function for RF regression was the same as the RF classifier model.  
197 Temperature, previous O<sub>3</sub> observation, PBL height or relative humidity, were the selected features  
198 for the first phase RF regression model, and the temperature and hour were selected for the second  
199 phase.

200

## 201 **3.2. Machine learning model evaluation**

202 Cross-validation is commonly used for model evaluation, since it can test the subset of the dataset  
203 with an equal chance.<sup>34</sup> There are various cross-validation methods, such as leave-one-out, k-fold,  
204 etc. Here, the 10-time 10-fold and walk-forward cross-validation were used to evaluate the two  
205 modeling frameworks. The input data were the primary WRF output, time information and  
206 historical O<sub>3</sub> observations in Kennewick.

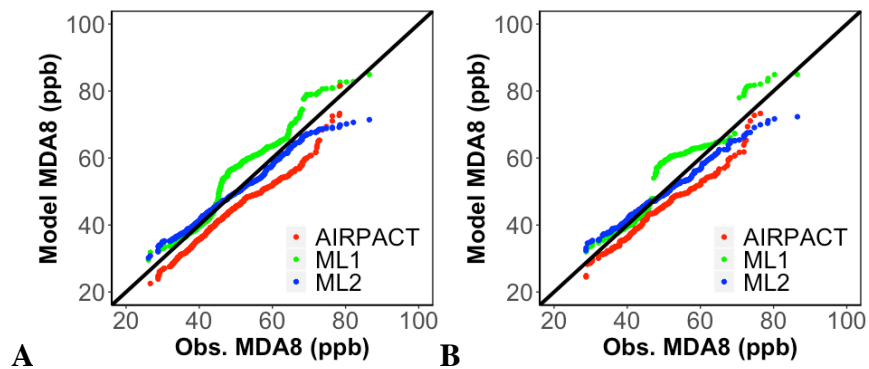
207

### 208 3.2.1 10-time 10-fold cross-validation

209 The k-fold cross-validation may be the most commonly used technique for the model evaluation.<sup>34</sup>  
210 It divides the dataset into k randomly chosen parts (k=10 in this research), and k-1 parts are used  
211 to train the model, the remaining portion is used to test the model, and this process is repeated k  
212 times to test all k subsets. The *RepeatedKfold* function in the python module *sklearn* was used to  
213 separate the dataset. To avoid any bias from data separation, the k-fold cross-validation was  
214 repeated 10 times in this research.

215 The NMB for these 10-time cross-validation was  $6.3\% \pm 0.2\%$  for ML1 and  $0 \pm 0.1\%$  for ML2.  
216 The AIRPACT NMB was  $-9.3\%$ , which was lower than ML1 and ML2. The standard deviations  
217 show that there is no significant difference among each repeat, and the model performance is  
218 stable.

219 The Q-Q plots in Figure 2A show the comparison between the model predictions and  
220 observations. AIRPACT underpredicted the MDA8 for MDA8 lower than 70 ppb. For MDA8  
221 higher than 70 ppb, AIRPACT tended to predict the DMA8 close to the 1:1 line, but there were  
222 several extremely high predictions from AIRPACT which were not shown in Figure 2A. ML1 and  
223 ML2 were close to the 1:1 line when the MDA8 was lower than 45 ppb. ML1 was close to the 1:1  
224 line for MDA8 in the 60 – 70 ppb range. For high MDA8 cases ( $> 70$  ppb), ML1 showed the best  
225 performance.

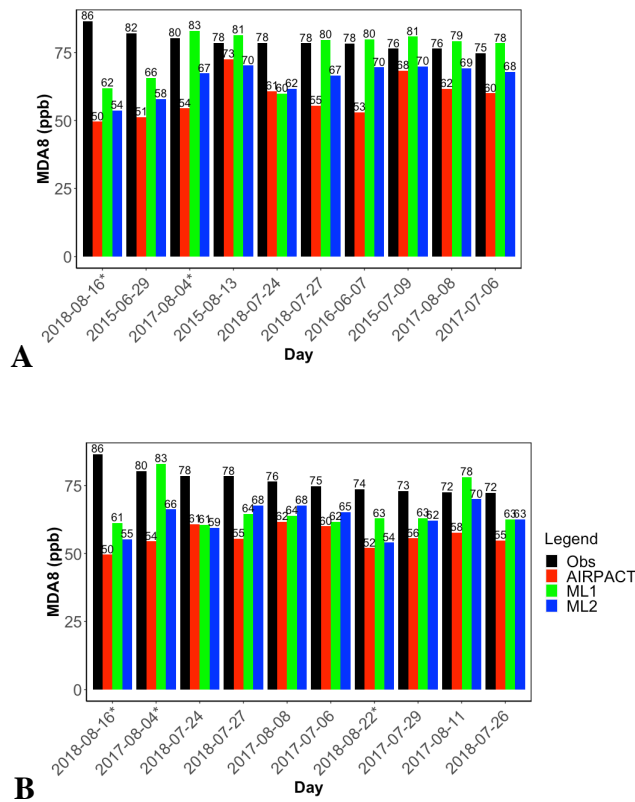


226 **Figure 2.** Q-Q plots of averaged model vs. observed MDA8 (A) during May – September 2015 –  
227 2018 based on the 10 times 10-fold cross-validation (B) during May – September 2017 – 2018  
228 based on the walk-forward cross-validation  
229

230  
231 The highest 10 observed MDA8 during 2015 – 2018 and their model predictions were selected  
232 and shown in Figure 2B. ML2 and AIRPACT underpredicted all 10 cases, and ML1 provided

233 close predictions for 7 out of 10. These results show that ML1 performs better for high O<sub>3</sub> events,  
 234 and results from the Q-Q plot also confirms this. The two ML models showed a similar trend,  
 235 and they both largely underpredicted 3 cases. So, they may miss the same factor which led to the  
 236 high MDA8. The highest O<sub>3</sub> day was affected by the wildfire smoke, and all models missed it.

237



238

239 **Figure 3.** Top 10 observed MDA8 and model predictions from (A) 10-time 10-fold cross-  
 240 validation (B) the walk-forward cross-validation

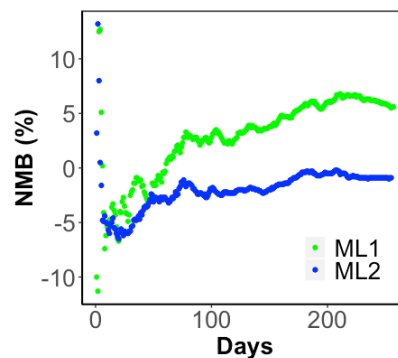
241 \* means that the wildfire smoke caused excess ozone on that day

242

243 3.2.2 Walk-forward cross-validation

244 The 10-time 10-fold cross-validation does not consider the temporal order of the data,  
245 which is important for the time-series data. Walk-forward cross-validation is a technique for time-  
246 series data.<sup>35</sup> For this evaluation, the 2015 and 2016 data were used to train the model and predict  
247 the first day in the 2017 dataset (May 1<sup>st</sup>, 2017). Then the May 1<sup>st</sup>, 2017 data was included in the  
248 training dataset and the models were used to predict O<sub>3</sub> for May 2<sup>nd</sup>, 2017. This process was  
249 repeated for each additional day of the 2017 and 2018 ozone seasons.

250 When a new day's MDA8 was predicted by the ML models, the NMB was recomputed by  
251 including the new prediction. The change of NMB was shown in Figure 3A. In the beginning,  
252 there was no clear trend for the NMB values for both ML models. The NMB from ML1 prediction  
253 sharply increased after June 2017 (Day 50 in Figure 3A) when more high O<sub>3</sub> events occurred,  
254 slowly increased after August 2017 (Day 100 in Figure 3A), and slowly decreased after July 2018  
255 (Day 200 in Figure 3A). The overprediction from ML1 during the low O<sub>3</sub> periods (May and June)  
256 could lead to the NMB increasing, while the NMB values were stable or even decreasing during  
257 the high O<sub>3</sub> period (July and August). For ML2, there were some fluctuations before August 2018,  
258 and the NMB was stable after that. For both ML1 and ML2, the NMB values were getting stable  
259 when more data got involved. The final NMB of two ML models were 5.6% and -0.9%, which  
260 were lower than the 10-time 10-fold cross-validation.



261  
262 **Figure 4.** The walk-forward NMB of each time step for ML1 and ML2

263

264 The walk-forward cross-validation provided two-year MDA8 predictions (2017 and 2018), and  
265 the Q-Q plots were similar to the 10-time 10-fold cross-validation. The two breakpoints of ML1  
266 distribution were clearer in Figure 3B. Ten highest MDA8 in 2017 and 2018 were shown in Figure  
267 4. ML1 only captures 2 out of the top 10 observed MDA8 and ML2 captured 1. In some cases,  
268 ML1 was even lower than ML2. Three high O<sub>3</sub> days with stars (\*) in Figure 4 were affected by the  
269 wildfire smoke, and ML1 captured two of them. The two ML models still performed better than  
270 AIRPACT.

271 Table 1 summarizes the HSS and KSS of the two machine learning models and AIRPACT from  
272 the two cross-validation methods. Both machine learning models show better performance with  
273 higher HSS and KSS values than AIRPACT. ML2 shows higher HSS than ML1 for both cross-  
274 validation results, which means ML2's prediction is generally more accurate. ML1 shows higher  
275 KSS in 10-time 10-fold cross-validation due to its better performance of high O<sub>3</sub> predictions. The  
276 statistics from AIRPACT and ML2 are close between two cross-validations, but HSS and KSS  
277 from walk-forward are lower than 10-time 10-fold cross-validation.

278 **Table 1. HSS and KSS from two cross-validations**

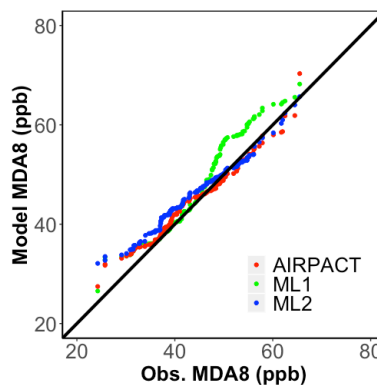
		AIRPACT	ML1	ML2
10-time 10-fold	HSS	0.32	0.44	0.55
	KSS	0.25	0.62	0.50
Walk-forward	HSS	0.34	0.37	0.57
	KSS	0.27	0.53	0.51

279



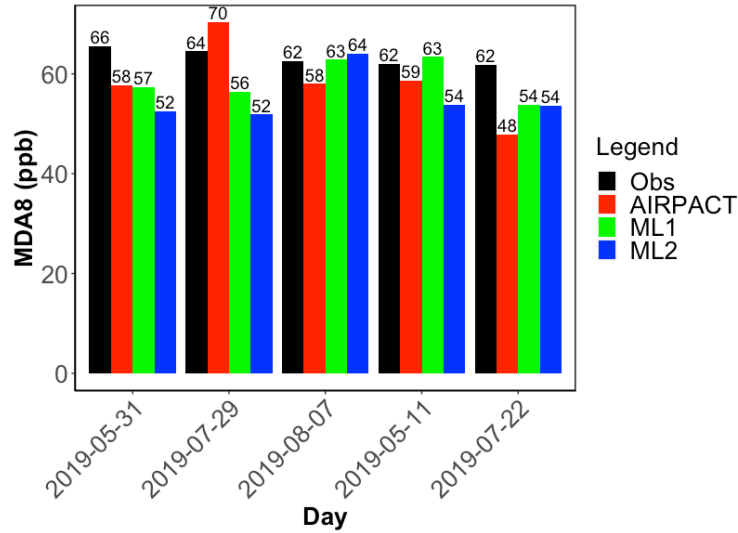
280 **3.3. O<sub>3</sub> ensemble forecasting in 2019**

281 Since April 2019, our machine learning models have been used for operational O<sub>3</sub> ensemble  
282 forecasting for Kennewick, WA. The ensemble forecasting to predict O<sub>3</sub> levels was based on more  
283 than 20 WRF ensemble members provided by the University of Washington. The difference  
284 among the predicted MDA8 from the ensemble members was not significant (within 5%). To better  
285 compare with the evaluation in the previous section, this section only covers the data from May to  
286 September in 2019. The ML1 and ML2 results are the ensemble means of the MDA8 values from  
287 more than 20 ML forecasts. The Q-Q plot in Figure 5 shows that the ML1, ML2 and AIRPACT  
288 model forecasts are close for O<sub>3</sub> lower than 40 ppb. For the O<sub>3</sub> in 40 – 60 ppb, ML1 tends to  
289 overpredict, while AIRPACT and ML2 are closer to observations. When the O<sub>3</sub> mixing ratio is  
290 higher than 60 ppb, ML1 slightly overpredicts, ML2 underpredicts, and AIRPACT varies in cases.  
291 For the highest 5 MDA8 points in Figure 6, the observed values were 62 – 66 ppb, while ML1’s  
292 predictions were closer to the observations than AIRPACT and ML2. AIRPACT showed larger  
293 variation (48 – 70 ppb) compared to two ML models.



294

295 **Figure 5.** Q-Q plots of ensemble mean model vs. observed MDA8 during May - September 2019

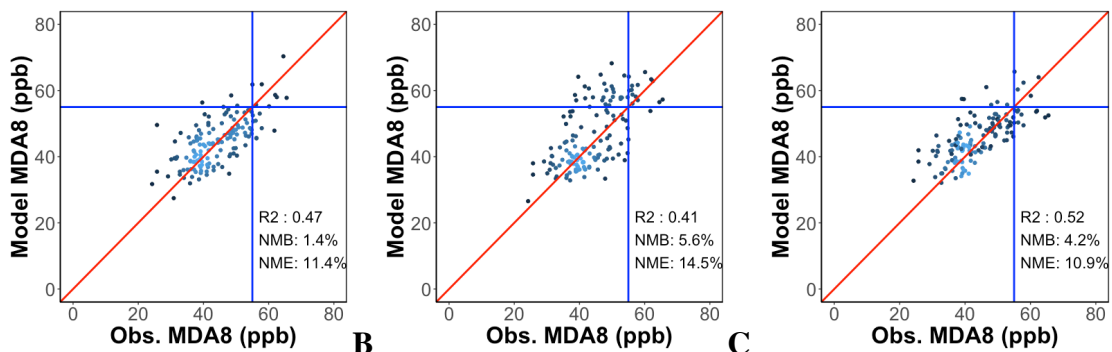


296

297 **Figure 6.** Top 5 observed MDA8 and model predictions in 2019

298

299 The scatter plots in Figure 7 show the ensemble mean MDA8 from May to September in 2019.  
 300 ML2 shows relatively higher  $R^2$  value (0.52) than ML1 (0.41) and AIRPACT (0.47). The NMB of  
 301 AIRPACT is lowest (1.4%), but its NME (11.4%) is higher than ML2 (10.9%). The low NMB is  
 302 due to the offset of overprediction and underprediction. ML1 tended to overpredict the MDA8  $O_3$   
 303 especially when it was higher than 40 ppb. Because of mostly favorable meteorological conditions  
 304 and few wildfires in the Pacific Northwest, the  $O_3$  mixing ratios were not very high in 2019 and  
 305 the model performance of ML2 was the best.



306

A

B

C

307 **Figure 7.** Scatter plots of observed vs. ensemble mean MDA8 of AIRPACT in (A), ML1 in (B)  
 308 and ML2 in (C) at Kennewick from May to September in 2019

309

310 The model performance statistics are presented in Table 2, the blue cells show misses, and red  
 311 cells show false alarms. In 2019, all the AQI<sub>obs</sub> at Kennewick were less than 3. Compared to  
 312 AIRPACT, ML1 captured high O<sub>3</sub> days better (15 events vs. 7 events for AQI<sub>obs</sub>2) but tended to  
 313 overpredict the O<sub>3</sub> AQI (26 false alarm events vs. 3 false alarm events). ML2 predicted similar  
 314 AQI days to AIRPACT. Based on the analysis above, we decided to use ML1 to provide the daily  
 315 forecasting for Kennewick when the predicted AQI was above 2, and ML2 when the predicted  
 316 AQI was 1 or 2.

317 **Table 2. Number of days for each AQI during May – September 2019**

		Observation								
		AQI 1		AQI 2		AQI 1		AQI 2		
AQI 2	AQI 1	AIRPACT	122	11	ML1	99	3	ML2	119	13
			3	7		26	15		6	5

318 ML1 and ML2 are the ensemble mean results using 20 WRF ensemble members.

319 The blue cells mean the model misses high O<sub>3</sub>, and the red cells mean the model raises false  
 320 alarms.

321

322 **Acknowledgement**

323 We thank the fund from CEE - YUNHA LEE ACCRUALS (2315-0028). We acknowledge that

324 David Ovens from University of Washington helped setup a data feed of WRF ensembles.

325 **Reference:**

- 326 (1) Sportisse, B. A Review of Current Issues in Air Pollution Modeling and Simulation.  
327 *Computational Geosciences* **2007**, *11* (2), 159–181. <https://doi.org/10.1007/s10596-006-9036-4>.
- 328 (2) Seinfeld, J. H.; Pandis, S. N. *Atmospheric Chemistry and Physics: From Air Pollution to*  
329 *Climate Change*; John Wiley & Sons, 2016.
- 330 (3) April 1, 2019 Population of Cities, Towns and Counties Used for Allocation of Selected  
331 State Revenues State of Washington. Washington State Office of Financial Management 2019.
- 332 (4) B. T. Jobson; G. VanderSchelden. *The Tri-Cities Ozone Precursor Study (T-COPS)*; Final  
333 Report; Washington Department of Ecology, 2017.
- 334 (5) Feng, X.; Li, Q.; Zhu, Y.; Hou, J.; Jin, L.; Wang, J. Artificial Neural Networks Forecasting  
335 of PM<sub>2.5</sub> Pollution Using Air Mass Trajectory Based Geographic Model and Wavelet  
336 Transformation. *Atmospheric Environment* **2015**, *107*, 118–128.  
337 <https://doi.org/10.1016/j.atmosenv.2015.02.030>.
- 338 (6) Freeman, B. S.; Taylor, G.; Gharabaghi, B.; Thé, J. Forecasting Air Quality Time Series  
339 Using Deep Learning. *Journal of the Air & Waste Management Association* **2018**, *68* (8), 866–  
340 886. <https://doi.org/10.1080/10962247.2018.1459956>.
- 341 (7) Zamani Joharestani, M.; Cao, C.; Ni, X.; Bashir, B.; Talebiesfandarani, S. PM<sub>2.5</sub>  
342 Prediction Based on Random Forest, XGBoost, and Deep Learning Using Multisource Remote  
343 Sensing Data. *Atmosphere* **2019**, *10* (7), 373. <https://doi.org/10.3390/atmos10070373>.

- 344 (8) Delavar, M.; Gholami, A.; Shiran, G.; Rashidi, Y.; Nakhaeizadeh, G.; Fedra, K.; Hatefi  
345 Afshar, S. A Novel Method for Improving Air Pollution Prediction Based on Machine Learning  
346 Approaches: A Case Study Applied to the Capital City of Tehran. *ISPRS International Journal of*  
347 *Geo-Information* **2019**, *8* (2), 99. <https://doi.org/10.3390/ijgi8020099>.
- 348 (9) Watson, G. L.; Telesca, D.; Reid, C. E.; Pfister, G. G.; Jerrett, M. Machine Learning  
349 Models Accurately Predict Ozone Exposure during Wildfire Events. *Environmental Pollution*  
350 **2019**, *254*, 112792. <https://doi.org/10.1016/j.envpol.2019.06.088>.
- 351 (10) Zheng, Y.; Liu, F.; Hsieh, H.-P. U-Air: When Urban Air Quality Inference Meets Big Data.  
352 In *Proceedings of the 19th ACM SIGKDD international conference on Knowledge discovery and*  
353 *data mining - KDD '13*; ACM Press: Chicago, Illinois, USA, 2013; p 1436.  
354 <https://doi.org/10.1145/2487575.2488188>.
- 355 (11) Pernak, R.; Alvarado, M.; Lonsdale, C.; Mountain, M.; Hegarty, J.; Nehr Korn, T.  
356 Forecasting Surface O<sub>3</sub> in Texas Urban Areas Using Random Forest and Generalized Additive  
357 Models. *Aerosol Air Qual. Res.* **2019**, *9* (12), 2815–2826.  
358 <https://doi.org/10.4209/aaqr.2018.12.0464>.
- 359 (12) Rybarczyk, Y.; Zalakeviciute, R. Machine Learning Approaches for Outdoor Air Quality  
360 Modelling: A Systematic Review. *Applied Sciences* **2018**, *8* (12), 2570.  
361 <https://doi.org/10.3390/app8122570>.
- 362 (13) Yu, R.; Yang, Y.; Yang, L.; Han, G.; Move, O. RAQ-A Random Forest Approach for  
363 Predicting Air Quality in Urban Sensing Systems. *Sensors* **2016**, *16* (1), 86.  
364 <https://doi.org/10.3390/s16010086>.

- 365 (14) Zhan, Y.; Luo, Y.; Deng, X.; Grieneisen, M. L.; Zhang, M.; Di, B. Spatiotemporal  
366 Prediction of Daily Ambient Ozone Levels across China Using Random Forest for Human  
367 Exposure Assessment. *Environmental Pollution* **2018**, *233*, 464–473.  
368 <https://doi.org/10.1016/j.envpol.2017.10.029>.
- 369 (15) Breiman, L. Random Forests. *Machine Learning* **2001**, *45* (1), 5–32.  
370 <https://doi.org/10.1023/A:1010933404324>.
- 371 (16) Kam, H. T. Random Decision Forest. In *Proceedings of the 3rd International Conference*  
372 *on Document Analysis and Recognition*; 1995; Vol. 1416, p 278282.
- 373 (17) Mitchell, T. M. *Machine Learning*; McGraw-Hill series in computer science; McGraw-  
374 Hill: New York, 1997.
- 375 (18) Arganis, M. L.; Val, R.; Dominguez, R.; Rodriguez, K.; Dolz, J.; Eato, J. M. Comparison  
376 Between Equations Obtained by Means of Multiple Linear Regression and Genetic Programming  
377 to Approach Measured Climatic Data in a River. In *Genetic Programming - New Approaches and*  
378 *Successful Applications*; Ventura Soto, S., Ed.; InTech, 2012. <https://doi.org/10.5772/50556>.
- 379 (19) Chaloulakou, A.; Assimacopoulos, D.; Lekkas, T. Forecasting Daily Maximum Ozone  
380 Concentrations in the Athens Basin. 16.
- 381 (20) Moustris, K. P.; Nastos, P. T.; Larissi, I. K.; Paliatsos, A. G. Application of Multiple Linear  
382 Regression Models and Artificial Neural Networks on the Surface Ozone Forecast in the Greater  
383 Athens Area, Greece. *Advances in Meteorology* **2012**, *2012*, 1–8.  
384 <https://doi.org/10.1155/2012/894714>.

385 (21) Sousa, S.; Martins, F.; Alvimferraz, M.; Pereira, M. Multiple Linear Regression and  
386 Artificial Neural Networks Based on Principal Components to Predict Ozone Concentrations.  
387 *Environmental Modelling & Software* **2007**, *22* (1), 97–103.  
388 <https://doi.org/10.1016/j.envsoft.2005.12.002>.

389 (22) Yuchi, W.; Gombojav, E.; Boldbaatar, B.; Galsuren, J.; Enkhmaa, S.; Beejin, B.; Naidan,  
390 G.; Ochir, C.; Legtseg, B.; Byambaa, T.; Barn, P.; Henderson, S. B.; Janes, C. R.; Lanphear, B. P.;  
391 McCandless, L. C.; Takaro, T. K.; Venners, S. A.; Webster, G. M.; Allen, R. W. Evaluation of  
392 Random Forest Regression and Multiple Linear Regression for Predicting Indoor Fine Particulate  
393 Matter Concentrations in a Highly Polluted City. *Environmental Pollution* **2019**, *245*, 746–753.  
394 <https://doi.org/10.1016/j.envpol.2018.11.034>.

395 (23) Weaver, C. P.; Liang, X.-Z.; Zhu, J.; Adams, P. J.; Amar, P.; Avise, J.; Caughey, M.; Chen,  
396 J.; Cohen, R. C.; Cooter, E.; Dawson, J. P.; Gilliam, R.; Gilliland, A.; Goldstein, A. H.; Grambsch,  
397 A.; Grano, D.; Guenther, A.; Gustafson, W. I.; Harley, R. A.; He, S.; Hemming, B.; Hogrefe, C.;  
398 Huang, H.-C.; Hunt, S. W.; Jacob, D. J.; Kinney, P. L.; Kunkel, K.; Lamarque, J.-F.; Lamb, B.;  
399 Larkin, N. K.; Leung, L. R.; Liao, K.-J.; Lin, J.-T.; Lynn, B. H.; Manomaiphiboon, K.; Mass, C.;  
400 McKenzie, D.; Mickley, L. J.; O’neill, S. M.; Nolte, C.; Pandis, S. N.; Racherla, P. N.; Rosenzweig,  
401 C.; Russell, A. G.; Salathé, E.; Steiner, A. L.; Tagaris, E.; Tao, Z.; Tonse, S.; Wiedinmyer, C.;  
402 Williams, A.; Winner, D. A.; Woo, J.-H.; Wu, S.; Wuebbles, D. J. A Preliminary Synthesis of  
403 Modeled Climate Change Impacts on U.S. Regional Ozone Concentrations. *Bull. Amer. Meteor.*  
404 *Soc.* **2009**, *90* (12), 1843–1864. <https://doi.org/10.1175/2009BAMS2568.1>.



- 405 (24) Gong, X.; Kaulfus, A.; Nair, U.; Jaffe, D. A. Quantifying O<sub>3</sub> Impacts in Urban Areas Due  
406 to Wildfires Using a Generalized Additive Model. *Environ. Sci. Technol.* **2017**, *51* (22), 13216–  
407 13223. <https://doi.org/10.1021/acs.est.7b03130>.
- 408 (25) Mass, C. F.; Albright, M.; Ovens, D.; Steed, R.; Maciver, M.; Gritmit, E.; Eckel, T.; Lamb,  
409 B.; Vaughan, J.; Westrick, K.; Storck, P.; Colman, B.; Hill, C.; Maykut, N.; Gilroy, M.; Ferguson,  
410 S. A.; Yetter, J.; Sierchio, J. M.; Bowman, C.; Stender, R.; Wilson, R.; Brown, W. Regional  
411 Environmental Prediction Over the Pacific Northwest. *Bull. Amer. Meteor. Soc.* **2003**, *84* (10),  
412 1353–1366. <https://doi.org/10.1175/BAMS-84-10-1353>.
- 413 (26) Pacific Northwest Environmental Forecasts and Observations  
414 <https://a.atmos.washington.edu/mm5rt/> (accessed Mar 6, 2020).
- 415 (27) Haixiang, G.; Yijing, L.; Shang, J.; Mingyun, G.; Yuanyue, H.; Bing, G. Learning from  
416 Class-Imbalanced Data: Review of Methods and Applications. *Expert Systems with Applications*  
417 **2017**, *73*, 220–239. <https://doi.org/10.1016/j.eswa.2016.12.035>.
- 418 (28) Jiang, N.; Riley, M. L. Exploring the Utility of the Random Forest Method for Forecasting  
419 Ozone Pollution in SYDNEY. **2015**, *1* (5), 10.
- 420 (29) Ukkonen, P.; Manzato, A.; Mäkelä, A. Evaluation of Thunderstorm Predictors for Finland  
421 Using Reanalyses and Neural Networks. *J. Appl. Meteor. Climatol.* **2017**, *56* (8), 2335–2352.  
422 <https://doi.org/10.1175/JAMC-D-16-0361.1>.
- 423 (30) Jolliffe, I. T.; Stephenson, D. B. *Forecast Verification: A Practitioner's Guide in*  
424 *Atmospheric Science*; John Wiley & Sons, 2012.

- 425 (31) Wilks, D. S. *Statistical Methods in the Atmospheric Sciences*; Academic press, 2011; Vol.  
426 100.
- 427 (32) Doswell III, C. A.; Davies-Jones, R.; Keller, D. L. On Summary Measures of Skill in Rare  
428 Event Forecasting Based on Contingency Tables. *Weather and Forecasting* **1990**, 5 (4), 576–585.
- 429 (33) Murphy, K. P. *Machine Learning: A Probabilistic Perspective*; MIT press, 2012.
- 430 (34) Raschka, S. Model Evaluation, Model Selection, and Algorithm Selection in Machine  
431 Learning. *arXiv:1811.12808 [cs, stat]* **2018**.
- 432 (35) Falessi, D.; Narayana, L.; Thai, J. F.; Turhan, B. Preserving Order of Data When Validating  
433 Defect Prediction Models. 20.